

Time Delay Margin Analysis for an Adaptive Controller

Andrei Dorobantu*, Peter Seiler†, and Gary J. Balas‡

Department of Aerospace Engineering & Mechanics

University of Minnesota, Minneapolis, MN, 55455, USA

Adaptive control has the potential to improve performance and reliability in aircraft systems. Implementation of adaptive control on commercial and military aircraft requires verification and validation of the control system's robustness to modeling error, uncertainty, and time delay. Currently, there is a lack of tools available to rigorously analyze the robustness of adaptive controllers due to their inherently nonlinear dynamics. This article addresses the application of nonlinear robustness analysis tools to an adaptive flight control system. First, a model reference adaptive controller is derived for a linear aircraft short-period model. The resulting closed-loop system is nonlinear and governed by polynomial dynamics. Sum-of-squares polynomial optimization is applied to the closed-loop system to assess its robustness to time delay. Time delay margins are computed for various combinations of design parameters in the adaptive law, as well as in the presence of parametric model uncertainty.

I. Introduction

Adaptive control has the potential to improve performance and reliability in aircraft. However, typical adaptive control architectures are inherently nonlinear, which presents a set of new challenges. There is currently a lack of tools available to rigorously analyze the robustness and performance of such systems. The inability to verify robustness and performance is a significant roadblock to the implementation of adaptive control on civilian and military aircraft.

*PhD Candidate, AIAA Student Member, dorob002@aem.umn.edu

†Assistant Professor, AIAA Member, seiler@aem.umn.edu

‡Professor, AIAA Associate Fellow, balas@aem.umn.edu

Many nonlinear systems, including the adaptive control system considered in this article, are governed by polynomial dynamics. The primary objective of this paper is to demonstrate the suitability of sum-of-squares (SOS) polynomial optimization for the analysis of such adaptive flight control systems. There has recently been significant research on SOS optimization problems which have been used to analyze the performance and robustness of systems described by polynomial dynamics.¹⁻³ Computational algorithms have been developed for estimating regions of attraction, reachability sets, input-output gains, robustness with respect to uncertainty, and time delay margins.⁴⁻²⁰ Moreover, there is freely available software to solve SOS optimizations.²¹⁻²³

This article demonstrates that SOS polynomial optimization can be applied to assess the robustness of an adaptive flight control system to time delay. An important and meaningful robustness metric for nonlinear systems is the time delay margin. SOS optimization is used to calculate lower bounds on this robustness metric, and Monte Carlo simulations are used to calculate upper bounds. This approach was previously applied to a flight control system with model reference adaptive control (MRAC).²⁴⁻²⁶ This article extends that work by refining the optimization algorithms and analysis.

An MRAC is derived for the linear short-period dynamics of an aircraft in Section II. Section III briefly outlines the principles of SOS optimization. Section IV details the SOS optimization for time delayed systems and formulates a time delayed version of the closed-loop MRAC system. Section V summarizes the results of the time delay margin analysis, and Section VI provides concluding remarks.

II. Aircraft Model and Controller

The X-15 was an experimental hypersonic rocket propelled aircraft flown in the 1960s by NASA. One of the goals of the X-15 program was to flight test an implementation of adaptive control. An excellent source for more detail and information on the X-15's adaptive control program is found in Reference 27. As a result of this program, the model of the X-15 dynamics have served as a benchmark platform for adaptive control research and analysis. This section describes a linear model of the X-15 short-period dynamics implemented with a model reference adaptive controller. The aircraft model and controller are taken from Reference 28. This particular implementation of adaptive control was previously studied and analyzed for robustness using various techniques.^{24-26,28}

A. Short-Period Aircraft Model

A short-period model of the X-15 longitudinal dynamics is given by Equation 1.

$$\begin{aligned}\dot{x} &= A_\lambda x + Bu \\ y &= Cx\end{aligned}\tag{1}$$

The states of the system are angle-of-attack α (deg) and pitch rate q (deg/sec), given by $x = [\alpha, q]^\top$. The input to the system is elevator deflection $u = \delta_{elev}$ (deg), and the output is the angle-of-attack $y = \alpha$. The subscript λ on the state matrix A_λ denotes parametric uncertainty. The state, input, and output matrices for the X-15 short-period model are defined in Equations 2 - 4.

$$A_\lambda = \begin{bmatrix} -0.2950 & 1.0000 \\ -13.0798\lambda_\alpha & -0.2084\lambda_q \end{bmatrix}\tag{2}$$

$$B = \begin{bmatrix} 0 \\ -9.4725 \end{bmatrix}\tag{3}$$

$$C = \begin{bmatrix} 1 & 0 \end{bmatrix}\tag{4}$$

The aircraft model is denoted P_λ , indicating that it is an uncertain system. The terms λ_α and λ_q model parametric uncertainty in two aerodynamic coefficients.²⁹ Defining an appropriate parameter space for the uncertainty is required for analysis. 75 % parametric uncertainty is considered by allowing the λ terms to vary on the interval $[\cdot 25, 1.75]$. The short-period dynamics remain stable throughout this uncertainty envelope.

The nominal state matrix is denoted A_{nom} and corresponds to $\lambda_\alpha = \lambda_q = 1$. Eigenvalue decomposition reveals that the nominal short-period mode has a damping ratio $\zeta = 0.07$ at a frequency $\omega_n = 3.63$ rad/sec. Hence, the short-period dynamics are lightly damped. One of the goals of the control design is to attenuate the oscillations corresponding to this mode.

B. Model Reference Adaptive Control

A model reference adaptive controller is applied to the X-15 short-period model. The MRAC is nonlinear and has four main components: a reference model, an adaptive law, and two constant gains. The closed-loop system interconnection is shown in Figure 1.

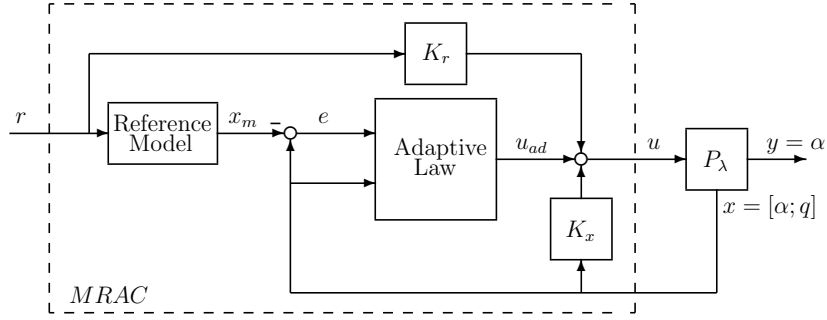


Figure 1. System interconnection for aircraft model with MRAC.

The interconnection shows that the control signal u is a summation of three signals. These signals originate from the state feedback gain K_x , the reference feedforward gain K_r , and the adaptive law. The resulting control signal u is the input to the aircraft model P_λ . Accordingly, the control law is defined by Equation 5.

$$u(t) = K_x x(t) + K_r r(t) + u_{ad}(t) \quad (5)$$

The state feedback gain K_x is designed first. Its objective is stability augmentation to increase damping in the short-period mode of the nominal model. The controller is designed using the LQR method with only the aircraft states, and minimizes the cost function J in Equation 6.

$$J = \int x(t)^T R_1 x(t) + u(t)^T R_2 u(t) dt \quad (6)$$

For the cost function J , the parameter weights R_1 and R_2 are selected as I_2 and 1, respectively. The resulting matrix K_x is shown in Equation 7.

$$K_x = \begin{bmatrix} 0.0577 & 0.9843 \end{bmatrix} \quad (7)$$

The inner-loop created by the stability augmentation system is overdamped with eigenvalues at -2.14 and -7.69. The nominal inner-loop transfer function $G_{il}(s)$ is given by Equation 8.

$$G_{il}(s) = C [sI_2 - (A_{nom} + BK_x)]^{-1} B \quad (8)$$

The feedforward gain K_r is designed such that the output of the nominal model y tracks the

input r at low frequency, and is defined with Equation 9.

$$K_r = G_{il}^{-1}(0) = [-C(A_{nom} + BK_x)^{-1}B]^{-1} = -1.7354 \quad (9)$$

Finally, the control signal u is augmented with u_{ad} , which corresponds to the adaptive law. This is the central feature of the controller. The adaptive law is defined in Equation 10.

$$u_{ad}(t) = \theta^T(t)x(t) \quad (10)$$

In this relationship, θ is a vector of adaptation parameters. The adaptation parameters are states of a virtual dynamic system, called the parameter update law and is defined in Equation 11.

$$\dot{\theta}(t) = -\kappa x(t)e^T(t)PB - \sigma\theta(t) \quad (11)$$

The error signal e is defined as the difference between the aircraft state x and the reference model state x_m . The reference model is equivalent to the nominal aircraft model in feedback with K_x and with K_r as a feedforward gain. In other words, the reference model is the transfer function $G_{il}(s)K_r$. The structure of the reference model is given in Equation 12.

$$\begin{aligned} \dot{x}_m &= (A_{nom} + BK_x)x_m + BK_r r \\ &:= A_m x_m + B_m r \\ y_m &= Cx_m \end{aligned} \quad (12)$$

The signal e is a characterization of the uncertain aircraft model's deviation from the nominal model. This deviation is the main driver in the parameter update law. If the aircraft model has no uncertainty, then x and x_m are identically equal to each other. In this case, θ decays as a function of time since the error is zero. Hence, adaptation is driven by uncertainty in the aircraft model.

There are two tuning parameters in the parameter update law. κ is the adaptation gain, and σ is the sigma modification gain. The adaptation gain determines how quickly the θ dynamics evolve. The sigma modification gain adds robustness to the system by ensuring boundedness of the θ parameters.

The symmetric matrix variable P is also a control design parameter. It is calculated by solving the Lyapunov equation $A_m^T P + P A_m = -Q$, where $Q = 2I_2$. The Lyapunov function $V = x^T P x$ can be used to prove stability for the MRAC closed-loop system when $\sigma = 0$. Further, Barbalat's lemma can show convergence of e to the origin. However, this analysis is no longer valid with the introduction of the sigma modification. The value of P used in

the control design is shown in Equation 13.

$$P = \begin{bmatrix} 1.8136 & 0.0341 \\ 0.0341 & 0.1085 \end{bmatrix} \quad (13)$$

The resulting closed-loop MRAC system is nonlinear. The adaptation parameters estimate uncertainty in the aircraft model, and feedback is used to drive the closed-loop dynamics towards the nominal condition. It is crucial to note that the closed-loop dynamics are polynomial, which is a requirement for SOS optimization. The nonlinearities are polynomial and only appear in the adaptive law (Equation 10) and in the parameter update law (Equation 11). The closed-loop state equations are summarized by Equations 14 - 16.

$$\dot{x} = (A_\lambda + BK_x)x + B\theta^T x + BK_r r \quad (14)$$

$$\dot{x}_m = A_m x_m + B_m r \quad (15)$$

$$\dot{\theta} = -\kappa x(x - x_m)^T P B - \sigma \theta \quad (16)$$

The following sections are focused on developing an approach that can be used to verify the robustness of this closed-loop system to time delay.

III. Sum-of-Squares Analysis

The underlying mathematical theory behind the time delay margin analysis in this article is related to properties of sum-of-squares (SOS) polynomials. This section provides a brief review of SOS polynomials and the optimizations that exploit their properties. Background and more detailed information can be found in References 1–3.

In general, a function $g(x)$ is a sum-of-squares polynomial if there exist polynomial functions f_1, \dots, f_n such that $g(x) = \sum_{i=1}^n f_i(x)^2$. For example, $g(x) = x_1^2 - 4x_1x_2 + 8x_2^2$ can be represented by $f_1 = x_1 - 2x_2$ and $f_2 = 2x_2$ as a sum of squared terms. A key property of SOS polynomials is that they are globally positive semidefinite. To check whether a polynomial is SOS, suppose that $g(x)$ is a polynomial of degree less than or equal to $2d$. Any such polynomial can be written in its vectorial decomposition, shown in Equation 17.

$$g(x) = c^\top w(x) \quad (17)$$

In this form, $w(x)$ is a vector of monomials in x of degree less than or equal to $2d$, and c is a unique vector of coefficients. For example, the polynomial $g(x) = x_1^2 - 4x_1x_2 + 8x_2^2$ can be represented by $c = [1, -4, 8]^\top$ and $w(x) = [x_1^2, x_1x_2, x_2^2]^\top$. On the other hand, the Gram

matrix representation of a polynomial is given by Equation 18.

$$g(x) = z^\top(x) Q z(x) \quad (18)$$

In the Gram matrix representation, $z(x)$ is a vector of monomials in x of degree less than or equal to d , and Q is a symmetric matrix. The polynomial $g(x) = x_1^2 - 4x_1x_2 + 8x_2^2$ can be represented in the Gram matrix form by $z(x) = [x_1, x_2]^\top$ and $Q = [1, -2; -2, 8]$. In general, a particular Gram matrix representation is not unique.

To parameterize all possible Gram matrix representations, a linear operator L is defined. Given any matrix Q , the polynomial $z^\top(x) Q z(x)$ can be formed and expressed uniquely in vector form as $c^\top w(x)$. Thus, given any symmetric matrix Q , the unique polynomial coefficients vector c can be computed. Define L as the operator mapping any symmetric matrix Q to a vector c , i.e. $L(Q) = c$. A matrix representation of L can be found since both its domain and range are finite dimensional. The transformation corresponding to L enables the parameterization of a family of symmetric matrices Q , shown in Equation 19, yielding Gram matrix representations of $g(x)$.

$$Q = Q_0 + \sum_{i=1}^s p_i N_i, \quad (19)$$

In this parametrization, Q_0 is any symmetric matrix corresponding to a particular Gram matrix representation of $g(x)$. The set $\{N_1, \dots, N_s\}$ is a basis of the null space of L , i.e. $L(N_i) = 0$. p is a vector of scalar multipliers. Any value of p in Equation 19 yields a valid Gram matrix representation of $g(x)$. A key mathematical result is that $g(x)$ is SOS if and only if it has a Gram matrix representation with a positive semidefinite matrix Q , denoted by $Q \succeq 0$.^{1,30} Consequently, $g(x)$ is SOS if and only if there exists a multiplier p for which $Q_0 + \sum_{i=1}^s p_i N_i \succeq 0$. This is a Linear Matrix Inequality (LMI) feasibility constraint that corresponds to an SOS constraint.

Many useful optimization problems can be formulated with SOS polynomials. An SOS program is an optimization problem with a linear cost and SOS constraints on the decision variables.²¹ SOS programs can be converted to semidefinite programs (SDPs) using the connection between SOS polynomials and positive semidefinite matrices. SOSOPT,²³ SOSTOOLS,²¹ and Yalmip²² are freely available MATLAB toolboxes for solving SOS optimizations. In particular, SOSOPT is used for the analysis in this article. SOSOPT allows the user to specify SOS constraints using an included polynomial toolbox. It converts the SOS optimization into an SDP, which is then solved with SeDuMi.^{31,32} Finally, the solution of the SDP is converted back to a polynomial solution.

SOS polynomials are globally positive semidefinite, which is a property that can be

exploited for the analysis of nonlinear systems. For example, SOS optimization can be used to construct a Lyapunov function that certifies the stability of a system. Lyapunov based stability analysis is generally centered around finding a positive definite function V whose derivative, with respect to time, is negative semidefinite. If the Lyapunov function candidate is restricted to be polynomial, then stability certificates can be obtained using an SOS optimization. This approach is ideally suited for control systems governed by polynomial dynamics, such as the MRAC system. For problems involving non-polynomial dynamics, the dynamics must be approximated as polynomials.

A significant limitation of SOS optimization is the rapid increase in the order of the resulting SDP as a function of the number of variables and the polynomial degree. For a generic degree $2d$ polynomial with n variables, the Gram matrix representation involves $l_z = \binom{n+d}{d}$ monomials in the vector $z(x)$. An SOS constraint is enforced via the positive semidefinite constraint on Q , which is an $l_z \times l_z$ Gram matrix. For example, Q has dimension $l_z = 495$ for a generic degree 8 polynomial in 8 variables and the null space of L has dimension $s = 109890$. The size of this matrix constraint is near the limits of current SDP solvers. The problem structure can be exploited,³³ but this computational growth is a generic trend in SOS optimizations. For analysis of polynomial systems, this roughly limits the approach to systems with fewer than 8-10 states and cubic degree models. Polynomial models of higher degree can be handled if there are fewer states.

Various types of nonlinear analysis problems have been formulated and analyzed in recent literature as SOS optimizations. Some of these include optimizations estimating regions of attraction, reachability sets, local input-output gains, input-output gains with other signal norms, robustness with respect to parametric uncertainty, and time delay margin.⁴⁻²⁰ The analysis in this article focuses on estimating the time delay margin for the MRAC system. SOS optimization is applicable because the MRAC closed-loop system is governed by polynomial dynamics.

IV. Time Delay Margin Analysis

An approach to calculating time delay margins for polynomial systems using SOS optimization was proposed in Reference 19, and refined in Reference 20. The approach in Reference 19 was used to analyze the MRAC system in References 24–26. The analysis in this article applies the refined approach in Reference 20 to improve upon the previous time delay margin results for the MRAC system.

In this section, a set of Lyapunov stability conditions is derived. These conditions can be used to prove stability of nonlinear systems with time delay. The conditions are subsequently relaxed, which allows them to be verified numerically via SOS optimization. Finally, the

MRAC closed-loop dynamics are formulated as a time delayed system, which can be analyzed for robustness with SOS optimization.

A. Stability Analysis for Nonlinear Time Delayed Systems

For the subsequent derivation, the time delayed closed-loop dynamics are restricted to the form in Equation 20.

$$\dot{x}(t) = f(x(t), x(t - \tau)) \quad (20)$$

In this model, $x(t) \in \mathbb{R}^n$ is the current state vector, $x(t - \tau) \in \mathbb{R}^n$ is the delayed state vector, and the origin is assumed to be an equilibrium point, i.e $f(0, 0) = 0$. Implicitly, this system is infinite dimensional. The current derivative depends explicitly on the current state and the delayed state. However, knowledge of the entire state time history on the time delay interval is required for predicting future states. This infinite dimensional state is denoted ϕ_t , where ϕ_t is the state at time t , which consists of the solution x defined in the entire interval $[t - \tau, t]$. Many real systems can be modeled this way, such as systems with controller computation, communication, or transport delay. The largest τ for which the equilibrium is stable is the time delay margin. The largest τ for which stability can be numerically certified is a lower bound on that margin.

A Lyapunov function candidate is proposed in Equation 21, which maps the infinite dimensional vector ϕ_t into a real number.¹⁹

$$V(\phi_t) = V_0(x(t)) + \int_0^r V_1(\tau, x(t), x(t - \tau)) d\tau + \int_0^r \int_{t-\tau}^t V_2(x(\xi)) d\xi, d\tau \quad (21)$$

One of the conditions of the Lyapunov stability theorem is that $V(\phi_t)$ be positive definite. Positive definiteness of each term in $V(\phi_t)$ is sufficient but not necessary. Given at least one positive definite term, the others can be positive semidefinite. V_0 is constrained to be positive definite by ensuring that it is greater than the function $\psi = x(t)^T x(t)$. This allows for slack in the remaining terms. The kernels V_1 and V_2 of the integral terms are constrained to be positive semi-definite. Indeed, the integral of a positive semi-definite function is positive semi-definite itself.

Another condition of the Lyapunov stability theorem is that the time derivative \dot{V} be negative semidefinite. It is lengthy, but straight-forward, to differentiate a Lyapunov candidate V of the form given in Equation 21. Details are provided in Reference 25. The resulting simplified form is shown in Equation 22. The kernel of this integral is constrained

to be negative semidefinite to certify stability of the time delayed system.

$$\begin{aligned} \frac{d}{dt}V = & \int_0^r \frac{1}{r} \frac{dV_o}{dx(t)} f + \frac{1}{r} V_1(r, x(t), x(t-r)) - \frac{1}{r} V_1(0, x(t), x(t)) \\ & + \frac{\partial V_1}{\partial x(t)} f - \frac{\partial V_1}{\partial \tau} + V_2(x(t)) - V_2(x(t-\tau)) d\tau \end{aligned} \quad (22)$$

A set of sufficient conditions that prove local stability of the time delayed system in Equation 20 is formulated in Lemma 1. For notational simplicity, the variables $x(t)$, $x(t-\tau)$, and $x(t-r)$ are replaced with x , y , and z , respectively. Conditions 1-3 ensure that V is positive definite and Condition 4 ensures that \dot{V} is negative semidefinite.

Lemma 1 *Assume the origin is an equilibrium point for the system in Equation 20 and let $\psi(x)$ be a given positive definite function. If there exist functions V_0 , V_1 , and V_2 such that:*

- 1) $V_0(x) - \psi(x) \geq 0 \quad \forall x$
- 2) $V_1(\tau, x, y) \geq 0 \quad \forall x, \forall y, \forall \tau \in [0, r]$
- 3) $V_2(x) \geq 0 \quad \forall x$
- 4) $\frac{1}{r} \frac{dV_o}{dx} f(x, y) + \frac{1}{r} V_1(r, x, z) - \frac{1}{r} V_1(0, x, x) + \frac{\partial V_1}{\partial \tau} f(x, y) - \frac{\partial V_1}{\partial \tau} + V_2(x) - V_2(y) \leq 0 \quad \forall x, \forall y, \forall z, \forall \tau \in [0, r]$

then the origin is a locally stable equilibrium for time delays $\tau \leq r$.

The stability conditions in Lemma 1 apply to general nonlinear systems with time delay of the form in Equation 20. With several assumptions and constraint relaxations, SOS optimization can be used to construct the Lyapunov function and certify the stability conditions. The next subsection details these assumptions and the constraint relaxation process.

B. SOS Stability Analysis for Polynomial Time Delayed Systems

SOS optimization is limited to constraints on polynomial functions. Hence, the general nonlinear structure of the Lyapunov stability conditions described in Lemma 1 cannot be implemented directly. However, if the system dynamics are limited to polynomials and the constraints are relaxed to SOS constraints, then SOS optimization can be used to construct the Lyapunov function and certify the stability conditions. SOS analysis can thus be used to calculate a lower bound on the time delay margin for the system.

Conditions 2 and 4 in Lemma 1 impose positive semidefinite constraints on the interval $\tau \in [0, r]$. This is an infinite collection of positive semidefinite constraints, i.e. one constraint for each τ on the interval. Hence, Conditions 2 and 4 cannot be directly enforced

as SOS constraints. As a remedy, Conditions 2 and 4 are relaxed using a variant of the S-procedure. A special polynomial function $h(\tau) = \tau(\tau - r)$ is defined. This function is negative semidefinite on the interval $\tau \in [0, r]$, and positive definite elsewhere. In particular, Condition 2 is relaxed to an SOS constraint on the following function: $V_1(\tau, x, y) + p_1 h(\tau)$. p_1 is required to be SOS through a separate constraint. Note that enforcing $V_1 + p_1 h$ to be an SOS polynomial ensures that it is globally non-negative. By construction of p_1 and h , this implies that Condition 2 is satisfied for all $\tau \in [0, r]$. Condition 4 is similarly relaxed by augmenting a term $p_2 h$, where p_2 is also enforced to be SOS. The functions p_1 and p_2 are SOS multiplier functions that chosen by the optimization.

In general, certifying global stability for nonlinear systems is conservative. As a result, the analysis in this article is restricted to proving local stability. This is accomplished by enforcing the positive definite constraint on V and the negative semidefinite constraint on \dot{V} only on a local region in the state space. This local region is described with a multi-dimensional box. If the Lyapunov conditions hold inside a multi-dimensional box containing the origin, then there exists a local region of attraction. In particular, the largest level set of the Lyapunov function fully contained in the box is an invariant set. Hence, every trajectory originating from within that level set remains within the level set. It is crucial to note that although the stability conditions are satisfied for the entire box, only the largest level set of the Lyapunov function can be interpreted as a region of attraction for the system.

The magnitude of the box describing the local region is defined by $|x_i| \leq \zeta_i$, where ζ_i is a fixed number. Each x_i represents an individual state, and to allow flexibility, each direction is constrained independently in terms of ζ_i . Consider functions of the form shown in Equations 23 - 25.

$$h_{1i} = (x_i - \zeta_i) (x_i + \zeta_i) \tag{23}$$

$$h_{2i} = (y_i - \zeta_i) (y_i + \zeta_i) \tag{24}$$

$$h_{3i} = (z_i - \zeta_i) (z_i + \zeta_i) \tag{25}$$

These functions are negative semidefinite in the local region, i.e. inside the box, and positive definite elsewhere. Since x , y , and z are treated as separate sets of state variables in Conditions 1 - 4 in Lemma 1, three sets of h_{ji} functions are required. Each state variable set is denoted with the j index. The i index is reserved for the individual state in a particular variable set. The h_{ji} functions are used to relax the positive definite constraint on V and the negative semidefinite constraint on \dot{V} by modifying Conditions 1 and 4 through a variant of the S-procedure. In particular, Condition 1 is relaxed to an SOS constraint on the following function: $V_0(x) - \psi(x) + \sum_{i=1}^n q_{1i} h_{1i}$. The functions q_{1i} are SOS multiplier functions that chosen by the optimization. Note that enforcing $V_0 - \psi + \sum_{i=1}^n q_{1i} h_{1i}$ to be an SOS poly-

nomial ensures that it is globally non-negative. By construction of q_{1i} and h_{1i} , this implies that Condition 1 is satisfied for all $|x_i| \leq \zeta_i$. Condition 4 is similarly relaxed by augmenting a term $\sum_{i=1}^n (q_{1i}h_{1i} + q_{2i}h_{2i} + q_{3i}h_{3i})$. The resulting SOS constraints ensure that Conditions 1 - 4 are satisfied in the local region.

Finally, Conditions 2 and 4 are augmented with polynomial functions s_1 and s_2 , respectively. These functions are used to improve the calculation of lower bounds on time delay margin. Conditions 2 and 4 are formulated as constraints on integral kernels. To ensure that the inclusion of functions s_1 and s_2 have no impact on the Lyapunov function, equality constraints are enforced on the integrals of s_1 and s_2 , shown in Equation 26.

$$\int_0^r s_1(x, \tau) d\tau = \int_0^r s_2(x, z, \tau) d\tau = 0 \quad (26)$$

The resulting stability conditions are complicated algebraically, but can be verified with an SOS program. In this paper, the Matlab toolbox SOSOPT²³ is used for the optimization along with SeDuMi.³¹ SOS conditions for local stability of polynomial systems with time delay up to size r are summarized in Lemma 2.

Lemma 2 *Assume the origin is an equilibrium point for a polynomial system of the form in Equation 20 and let $\psi(x)$ be a positive definite function. If there exist polynomial functions $V_0, V_1, V_2, p_i, q_{ji}$, and s_i such that:*

- 1) $V_0(x) - \psi(x) + \sum_{i=1}^n q_{1i}h_{1i} + s_1$ is SOS
- 2) $V_1(\tau, x, y) + p_1h(\tau) + r_1$ is SOS
- 3) $V_2(x)$ is SOS
- 4) $-r \frac{\partial V_1}{\partial x} f(x, y) - \frac{dV_0}{dx} f(x, y) + r \frac{\partial V_1}{\partial \tau} - rV_2(x) + rV_2(y) - V_1(r, x, z) + V_1(0, x, x) + p_2h(\tau) + \sum_{i=1}^n (q_{1i}h_{1i} + q_{2i}h_{2i} + q_{3i}h_{3i}) + s_2$ is SOS
- 5) $\int_0^r s_1(x, \tau) = 0$
- 6) $\int_0^r s_2(x, z, \tau) = 0$
- 7) p_i, q_{ji} , and s_i are SOS

then the origin is a locally stable equilibrium for time delays $\tau \leq r$.

The SOS conditions in Lemma 2 can be directly implemented as an SOS program. The conditions certify that all trajectories originating from the largest level set of the Lyapunov function contained in the local box are stable for all time delays up to size r . The remaining task is to formulate the MRAC closed-loop dynamics as a time delayed polynomial system.

C. Time Delayed MRAC Closed-Loop Dynamics

A pure time delay of magnitude τ seconds is introduced in the closed-loop system dynamics between the controller and aircraft model. This time delay can be interpreted physically as a computation, sampling, or network delay. A single time delay is considered in the dynamic model of the closed-loop system for simplicity.

The SOS conditions Lemma 2 apply to systems of the form in Equation 20. A key point is that the polynomial closed-loop system must be autonomous. Hence, the input signal r in the MRAC closed-loop system is neglected to satisfy this condition. Neglecting the input signal may appear limiting for a nonlinear system, since the choice of input and its size can generally lead to degradation of stability margins. In the case of the MRAC system, however, analysis with the particular input choice $r = 0$ still leads to insightful results. If the autonomous system does not have sufficiently large stability margins, the time-varying system cannot meet robustness requirements either.

The absence of the input signal r alters the MRAC system dynamics. The effect of the feedforward gain K_r is completely eliminated. The reference model state x_m is also zero for all time. This implies that the error signal e is always equivalent to the true aircraft state x , which alters the parameter update law. The parameter update law, in the absence of the reference signal, is shown in Equation 27. Note that the adaptive term is governed by the quadratic term xx^T , instead of xe^T .

$$\dot{\theta} = -\kappa xx^T PB - \sigma \theta \quad (27)$$

The simplified system dynamics are represented by an updated interconnection shown in Figure 2. Although the system dynamics are different from the original MRAC, the new dynamics remain polynomial. Hence, the robustness of the closed-loop system can be analyzed with the proposed SOS optimization.

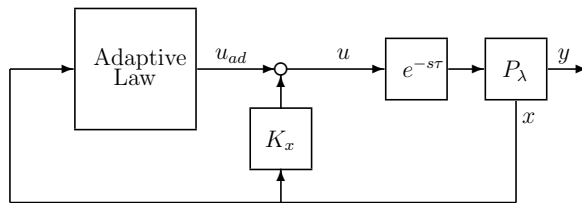


Figure 2. Simplified system interconnection neglecting input reference signal.

The SOS optimization certifies a set of local stability conditions for a box centered at the origin in the MRAC closed-loop system state space. Simulations of the nominal, undelayed system are used to guide the definition of this box in the locally stable region. For the

controller design, adaptation gain and sigma modification values of 1 are used. Simulations are initialized with the state $[\theta_1(0), \theta_2(0), \alpha(0), q(0)]^T = [0, 0, \alpha_o, q_o]^T$, where α_o and q_o are sampled along the rectangle formed by the local region box in $\alpha - q$ space. The results from simulations show that the locally stable region is at least ± 2 deg on α and ± 5 deg/sec on q . The locally stable region in the adaptation parameter space is at least ± 0.8 and ± 1.4 in θ_1 and θ_2 . However, to allow the consideration of adaptation rates greater than 1, a larger box in the adaptation parameter space is used. Simulations of the system with increased adaptation rate are used to guide this expansion, and a larger box defined by ± 1.6 and ± 4.5 in θ_1 and θ_2 is implemented. Together, four state space constraints form a four-dimensional box that is fully contained in the undelayed nonlinear system locally stable region. Note that simulations are only necessary to gain insight into the size of a physically meaningful box in state space of the closed-loop system.

SOS optimization is used to construct a Lyapunov function that is valid inside the box in the MRAC closed-loop system state space. However, this Lyapunov function does not prove that the entire box is a locally stable region. It is only guaranteed that V is positive definite, and that \dot{V} is negative semidefinite in the box. The guaranteed locally stable region is characterized by the largest level set fully contained in the box, and for time delays up to size r .

V. Results

The performance and robustness of a flight control law must be verified prior to implementation on military and commercial aircraft. One important step in certifying the robustness of a flight control law is to ensure that the closed-loop system meets a minimum time delay margin requirement. SOS optimization is used to find a lower bound on the time delay margin for the MRAC system. Monte Carlo simulations provide an upper bound. Since the exact margin is unknown, both the upper and lower bounds are needed for analysis. The SOS lower bound is meaningful if it lies above a required minimum value of time delay margin. In this case, the lower bound certifies that the flight control system meets the time delay margin requirement. Conversely, the Monte Carlo upper bound is meaningful if it falls below the requirement. In this case, the upper bound demonstrates that the time delay margin requirement is not satisfied. It cannot be determined if the minimum time delay margin is satisfied if the bounds straddle the requirement. In this case, however, the bounds can provide qualitative insight into trends in the time delay margin evaluated over a certain parameter space.

A reasonable minimum time delay margin requirement for the MRAC closed-loop system can be inferred from the open-loop aircraft model. The open-loop bandwidth is 5.6 rad/sec.

A typical performance and robustness phase margin requirement at the system bandwidth is 45 deg.³⁴ At 5.6 rad/sec, this requirement translates to a time delay margin of about 140 msec. Thus, a reasonable minimum time delay margin requirement for the MRAC closed-loop system is also 140 msec.

The parameter update law in the MRAC is tuned by adjusting adaptation rate and sigma modification. Tuning the parameter update law determines the adaptive contribution to the MRAC control signal. If the adaptive component is turned off, the MRAC becomes a linear system. Hence, the full closed-loop system is linear, and a precise time delay margin can be calculated. This time delay margin is calculated using the loop transfer function $L(s) = K_x P(s)$, in which the aircraft model is assumed to be nominal. With adaptation turned off, the time delay margin for the system is around 151 msec. This calculated margin exceeds the minimum requirement of 140 msec.

The calculation of time delay margin is desired for the MRAC closed-loop system with active adaptation. Trends in the time delay margin are found due to variations in the MRAC tuning parameters as well as for uncertainty in the aircraft model. The time delay margin results are interpreted in terms of trends in the upper and lower bounds, and the satisfaction of the minimum time delay margin requirement.

Subsection A focuses on the effect of varying adaptation rate. In this analysis, sigma modification is held constant to isolate the effect of changing adaptation rate. Subsection B focuses on the effect of varying sigma modification. In this analysis, adaptation rate is held constant to isolate the effect of changing sigma modification. The effect of uncertainty in the aircraft model is also examined. Changes in the aircraft dynamics are analyzed, and time delay margins are calculated over the uncertainty parameter space in Subsection C. Subsection D describes some of the computational limitations of time delay analysis using SOS optimizations..

A. Adaptation Rate

The effect of varying adaptation rate on the robustness of the MRAC closed-loop system is explored by analyzing the time delay margin. The sigma modification gain is constant at 1 for this analysis. An upper bound for the time delay margin is calculated using Monte Carlo simulations. In this process, random initial conditions are sampled along the boundary of the multi-dimensional box for increasing values of time delay. The upper bound is found with the lowest time delay that results in a divergent trajectory. The lower bound is calculated with SOS optimization.

The SOS lower bound proves that the origin is stable and, moreover, that there is an invariant set in the multi-dimensional local region. Since \dot{V} is negative semidefinite over the box, this invariant set is guaranteed to at least touch the boundary of the box. However,

since the invariant set does not necessarily contain the entire box, it is possible for there to exist a divergent trajectory emanating from inside the box. Thus it is possible for the SOS optimization to satisfy the Lyapunov stability conditions over the local box for a certain time delay τ and for the Monte Carlo sampling to find a divergent trajectory inside the box. Therefore, the upper and lower bounds are not precise complements of each other. Upper and lower bound time delay margin trends due to variations in adaptation rate are summarized in Figure 3.

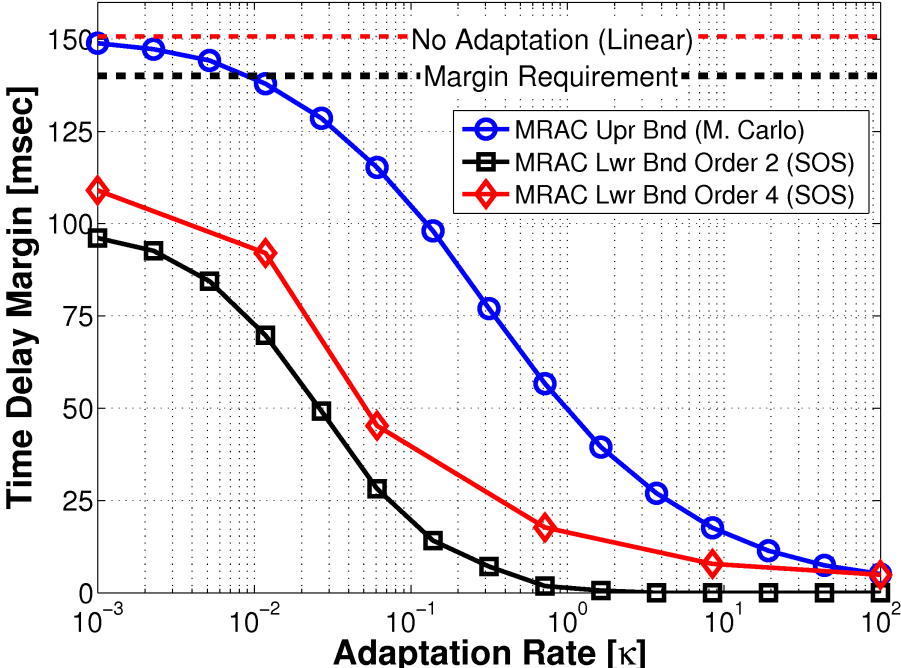


Figure 3. Time delay margin bounds as functions of adaptation rate.

The upper bound results confirm that decreasing adaptation rate κ leads to convergence of the closed-loop MRAC system to the linear inner-loop. This result is intuitive as decreasing κ effectively disables the adaptive law. For higher adaptation gains, the upper bound decreases. This result is also intuitive as higher bandwidth in controllers generally leads to a decrease in robustness to time delay. For values of κ larger than 0.01, the upper bound indicates that the minimum time delay margin requirement of 140 msec is no longer satisfied.

Two sets of SOS lower bounds are shown in Figure 3. The lowest bound, marked with squares, corresponds to solving the SOS optimization in Lemma 2 using second order polynomials. Solving this quadratic SOS program amounts to a reasonably large numerical problem with around 100 decision variables. On an average laptop with a dual-core processor and 4GB of RAM, a bisection algorithm with 9 iterations takes around 15 minutes to resolve a time delay margin value to a 1 msec accuracy. This lower bound is conservative compared to the upper bound. For low adaptation rates, the SOS optimization is able to numerically

certify that the adaptation rate is at least 94 msec. Although there is a significant gap between the bounds, the trend in decaying time delay margin is apparent.

The less conservative lower bound, marked with diamonds, corresponds to solving the SOS optimization in Lemma 2 by taking advantage of fourth order polynomials. For this calculation, the integral kernel portion V_1 of the Lyapunov function includes monomials up to degree 4. All other components remain quadratic. The use of higher order polynomials results in a less conservative lower bound on the time delay margin. However, the SOS program for the quartic case is significantly larger, with around 1500 decision variables. Including 4th order terms in V_1 increases the numerical size of the optimization more than tenfold. The quartic optimization can no longer be solved on an average laptop. Instead, a more powerful quad-core desktop with 6GB of RAM is used and takes around 3 hours to resolve a single iteration in the bisection sequence. More details on computational difficulties are provided in Subsection D on limitations of the SOS approach. The quartic SOS results decrease the gap between the upper and lower bounds. For the case of low adaptation rate, the lower bound certifies that the time delay margin is at least 110 msec.

Both lower bounds exhibit the same trend as the upper bound. The gap between the upper and lower bounds is significant for low adaptation rates, although it is reduced by considering higher order polynomials. The trend in the true time delay margin is apparent by considering both upper and lower bounds. Together, the bounds show that the time delay margin is highly sensitive to changes in the adaptation rate when $\kappa \in [0.01, 10]$. This is a region of interest for control because the adaptive law has a beneficial influence over the aircraft dynamics on this interval.²⁵ Although the MRAC does not satisfy the robustness requirements, the relationship between adaptation rate and time delay margin is revealed. Such insight cannot be drawn without the existence of both upper and lower bounds.

B. Sigma Modification

Time delay margin upper and lower bounds are calculated for varying sigma modification values. An adaptation rate of $\kappa = 1$ is held constant. The results in Figure 4 summarize the effect of varying sigma modification on the lower and upper bounds of time delay margin.

The upper bound in Figure 4 suggests that robustness to time delay increases with sigma modification. Further, it shows that the closed-loop system converges to the linear inner-loop for values of sigma larger than 1000. At this value, the adaptation is effectively turned off. It is impossible to design an MRAC that meets the 140 msec delay margin requirement with sigma modification less than 300. However, selecting such a high value greatly reduces the benefits of adaptation.

Two sets of SOS lower bounds are computed, similar to the case for varying adaptation rate. The quadratic results are shown by the more conservative lower bound marked with

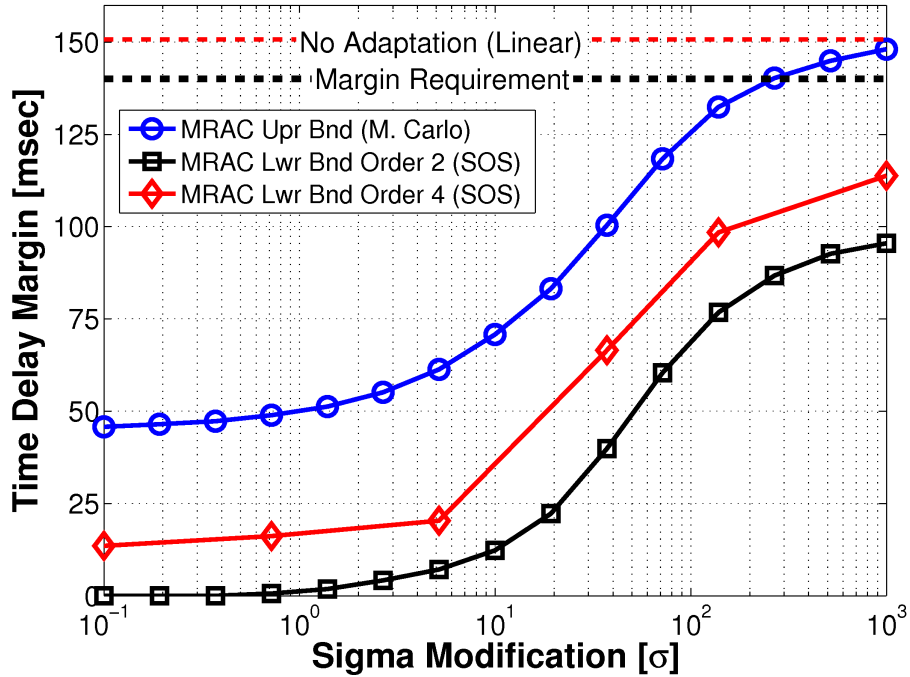


Figure 4. Time delay margin bounds as functions of sigma modification.

diamonds. The less conservative quartic results are marked with squares. Both lower bounds results exhibit a similar increasing trend to the upper bound. The bounds show a steep increasing trend for values of sigma between 10 and 100, and level out beyond 1000. Neither lower bound is able to show that the minimum time delay margin requirement is met for any value of sigma modification. However, they provides evidence that sigma modification cannot increase robustness without sacrificing performance in the adaptation.

The bounds in Figure 4 provide significant insight into the qualitative trend of the true time delay margin despite the lower bound being conservative. The bounds imply that the time delay margin is constant for very low and very high values of sigma modification. They also indicate the range of values for which the time delay margin is most sensitive to changes in sigma modification. Knowledge of such sensitivities is crucial in control design. This type of insight cannot be drawn from the upper bound alone since it does not provide any analytically rigorous results. However, in conjunction with a guaranteed lower bound, the qualitative trends can be interpreted with more confidence.

C. Aircraft Model Uncertainty

The use of adaptive control is motivated by the need to account for uncertainty in the aircraft model without sacrificing performance. The goal of MRAC is to ensure nominal aircraft performance in the presence of variations in the system dynamics. Uncertainty is

represented through the λ scaling parameters in the state matrix of the aircraft model. Each parameter varies on the interval $[0.25, 1.75]$ to encompass 75% uncertainty. A family of linear inner-loop transfer functions (neglecting feedforward gain K_r) from elevator input to angle-of-attack output is calculated for this interval by sampling the parameter space. Figure 5 shows the frequency response of this family of transfer functions to illustrate the effect of uncertainty on the aircraft dynamics.

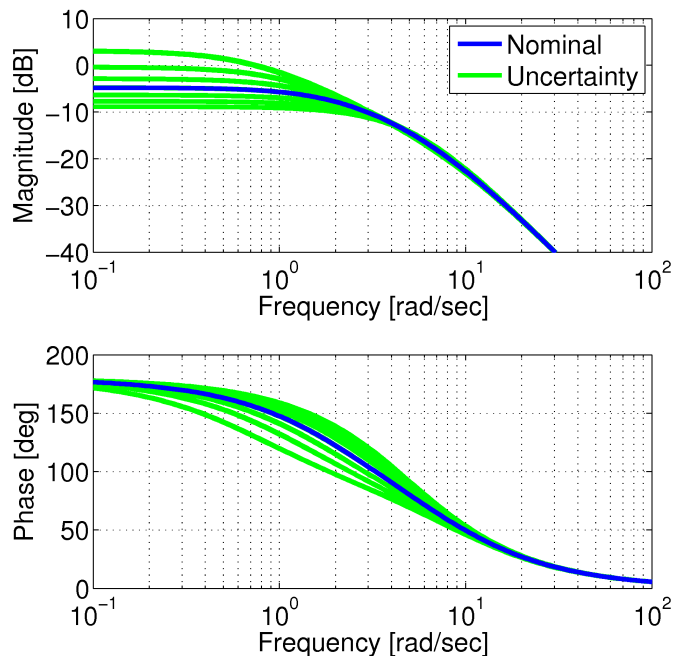


Figure 5. Inner-loop frequency response illustrating aircraft model uncertainty.

The results in Figure 5 suggest that uncertainty in the aircraft model is limited to changes in the low frequency characteristics of the inner-loop system. The nominal model is highlighted with the darker line on the plot. Deviations alter the DC gain of the system. The bandwidth of the system varies slightly, but this fluctuation does not affect the high frequency asymptote. This implies that the modes of the system do not vary independently due to uncertainty.

The dynamics of the closed-loop MRAC system are more sensitive to changes in λ_α than in λ_q . In the interest of computation time, λ_q is held fixed at its nominal value for this analysis. Time delay margins are calculated in the presence of 75 % uncertainty on λ_α to gain insight into its effect on robustness. An adaptation rate of 1 and a sigma modification value of 1 are selected for the adaptive law, supplying robustness without sacrificing performance in adaptation. Upper and lower bounds on the time delay margin are calculated with Monte Carlo simulations and SOS optimization, respectively. The results are summarized in Figure 6.

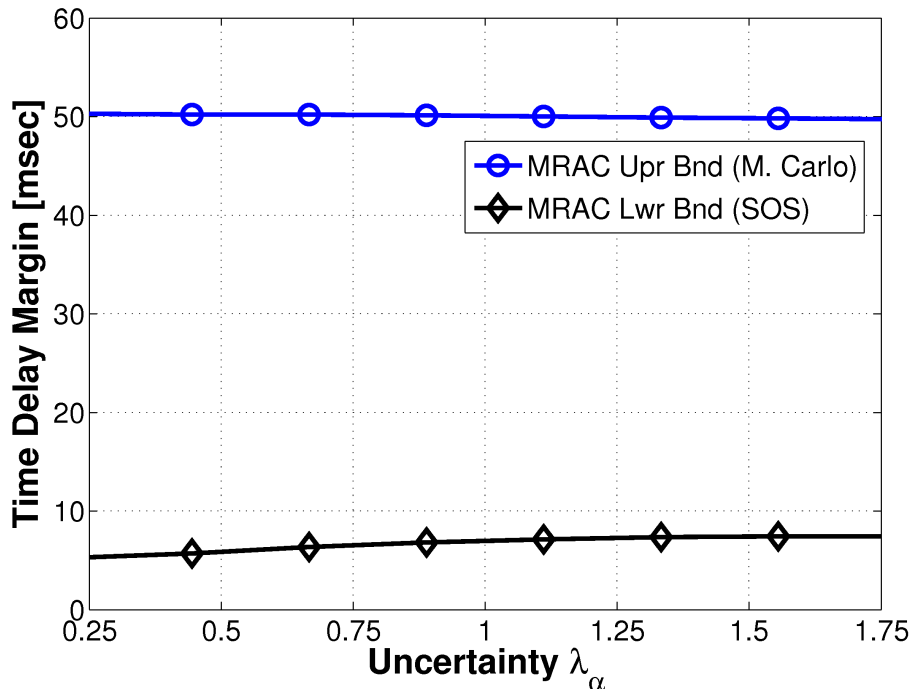


Figure 6. Time delay margin bounds as functions of aircraft model uncertainty.

The upper bound shown in Figure 6 shows that time delay margin is not sensitive to changes in the aircraft model due to parametric uncertainty. The lower bound is significantly more conservative, but confirms the same trend in the lack of sensitivity. The lower bound is computed using quadratic polynomials.

D. Limitations

A limitation of the SOS optimization for calculating time delay margin is a shortage of available memory and computation power. Due to the structure of the Lyapunov function, the dimension of the system of equations that must be analyzed is three times the dynamic order of the original system. Two extra sets of state variables are required to handle the time delay, resulting in a total of 12 states. The computational load of the SOS analysis grows with both the state order and the polynomial degree of the model. Hence, scaling the problem to larger systems is difficult, if not impossible, with current numerical algorithms and solvers.

The size of the SOS program with quartic polynomials is near the limit of currently available computation power. Extending this approach to more realistic, higher order systems will require new computational tools, including advances in SDP solvers and/or algorithms specifically tailored to SOS optimizations. In some cases with quartic Lyapunov functions, SeDuMi exhibits numerical issues in converging to a feasible result near the expected bound-

ary of the lower bound. As a result, the lower bound results for the quartic case are less continuous and exhibit jagged segments. However, even when SeDuMi exhibits numerical problems, the validity of the final result can easily be verified by checking that the constructed Lyapunov function satisfies the conditions in Lemma 2. Thus, it can be ensured that the results represent a true, however possibly sub-optimal, lower bound on the computed metric. The numerical issues prevent, in some cases, the computation of an optimal lower bound.

The solver’s ability to satisfy the SOS constraints is also sensitive to the dynamics of the system. State space and/or time scalings can be used to pre-condition the problem and reduce numerical issues. For the quartic SOS results presented in the previous sections, the dynamics were scaled spatially through a coordinate transformation normalizing the states according to the local region box. The dynamics were also scaled in time by a factor of ten to improve the numerical results. The use of state space and time transformations for numerical conditioning is common in commercial software³⁵ and needs further investigation for SOS analysis. Overall, the accuracy and efficiency of the SOS approach stands to benefit greatly from improvements in the numerical solvers of the optimization.

VI. Conclusion

This article used polynomial optimization techniques to calculate bounds on the time delay margin for an adaptive flight control system. These techniques were applied to a short-period aircraft model with model reference adaptive control. The results provide mathematically proven lower bounds on the time delay margin. The results also provide rigorous evidence for trends in the delay margin due to variations in the controller design. Although conservative, the results capture the time delay margin between upper and lower bounds that are relevant to engineering practice. Future work must focus on improving the numerical solvers and algorithms used in SOS optimizations to reduce the gap between upper and lower bounds.

Acknowledgments

This research was partially supported under the NASA Langley NRA contract NNH077ZEA001N entitled “Analytical Validation Tools for Safety Critical Systems” and the NASA Langley NRA Contract NNX08AC65A entitled “Fault Diagnosis, Prognosis and Reliable Flight Envelope Assessment.” The technical contract monitors are Dr. Christine Belcastro and Dr. Suresh Joshi, respectively. The research was also partially supported by the US National Science Foundation under Grant No. NSF-CNS-0931931.

References

- ¹Parrilo, P., *Structured Semidefinite Programs and Semialgebraic Geometry Methods in Robustness and Optimization*, Ph.D. thesis, California Institute of Technology, 2000.
- ²Lasserre, J., “Global Optimization with Polynomials and the Problem of Moments,” *SIAM Journal on Optimization*, Vol. 11, No. 3, 2001, pp. 796–817.
- ³Parrilo, P., “Semidefinite programming relaxations for semialgebraic problems,” *Mathematical Programming Ser. B*, Vol. 96, No. 2, 2003, pp. 293–320.
- ⁴Tibken, B., “Estimation of the domain of attraction for polynomial systems via LMIs,” *Proceedings of the IEEE Conference on Decision and Control*, 2000, pp. 3860–3864.
- ⁵Hachicho, O. and Tibken, B., “Estimating domains of attraction of a class of nonlinear dynamical systems with LMI methods based on the theory of moments,” *Proceedings of the IEEE Conference on Decision and Control*, 2002, pp. 3150–3155.
- ⁶Jarvis-Wloszek, Z., *Lyapunov Based Analysis and Controller Synthesis for Polynomial Systems using Sum-of-Squares Optimization*, Ph.D. thesis, University of California, Berkeley, 2003.
- ⁷Jarvis-Wloszek, Z., Feeley, R., Tan, W., Sun, K., and Packard, A., “Some Controls Applications of Sum of Squares Programming,” *Proceedings of the 42nd IEEE Conference on Decision and Control*, Vol. 5, 2003, pp. 4676–4681.
- ⁸Papachristodoulou, A., *Scalable analysis of nonlinear systems using convex optimization*, Ph.D. thesis, California Institute of Technology, 2005.
- ⁹Jarvis-Wloszek, Z., Feeley, R., Tan, W., Sun, K., and Packard, A., *Positive Polynomials in Control*, Vol. 312 of *Lecture Notes in Control and Information Sciences*, chap. Controls Applications of Sum of Squares Programming, Springer-Verlag, 2005, pp. 3–22.
- ¹⁰Chesi, G., Garulli, A., Tesi, A., and Vicino, A., “LMI-based computation of optimal quadratic Lyapunov functions for odd polynomial systems,” *International Journal of Robust and Nonlinear Control*, Vol. 15, 2005, pp. 35–49.
- ¹¹Prajna, S., *Optimization-Based Methods for Nonlinear and Hybrid Systems Verification*, Ph.D. thesis, California Institute of Technology, 2005.
- ¹²Tan, W., Packard, A., and Wheeler, T., “Local gain analysis of nonlinear systems,” *Proceedings of the American Control Conference*, 2006, pp. 92–96.
- ¹³Tan, W., *Nonlinear Control Analysis and Synthesis using Sum-of-Squares Programming*, Ph.D. thesis, University of California, Berkeley, 2006.
- ¹⁴Tibken, B. and Fan, Y., “Computing the domain of attraction for polynomial systems via BMI optimization methods,” *Proceedings of the American Control Conference*, 2006, pp. 117–122.
- ¹⁵Tan, W., Topcu, U., Seiler, P., Balas, G., and Packard, A., “Simulation-aided Reachability and Local Gain Analysis for Nonlinear Dynamical Systems,” *Proceedings of the IEEE Conference on Decision and Control*, 2008, pp. 4097–4102.
- ¹⁶Topcu, U., Packard, A., and Seiler, P., “Local stability analysis using simulations and sum-of-squares programming,” *Automatica*, Vol. 44, No. 10, 2008, pp. 2669–2675.
- ¹⁷Topcu, U., *Quantitative Local Analysis of Nonlinear Systems*, Ph.D. thesis, University of California, Berkeley, 2008.
- ¹⁸Topcu, U. and Packard, A., “Linearized Analysis Versus Optimization-based Nonlinear Analysis for Nonlinear systems,” *Proceedings of the American Control Conference*, 2009, pp. 790–795.

- ¹⁹Papachristodoulou, A., “Analysis of Nonlinear Time-Delay Systems using Sum of Squares Decomposition,” *Proceedings of the American Control Conference*, 2004, pp. 4153–4158.
- ²⁰Papachristodoulou, A., Peet, M., and Lall, S., “Analysis of Polynomial Systems With Time Delays via Sum of Squares Decomposition,” *IEEE Transactions on Automatic Control*, Vol. 54, No. 5, 2009, pp. 1058–1064.
- ²¹Prajna, S., Papachristodoulou, A., Seiler, P., and Parrilo, P. A., *SOSTOOLS: Sum of squares optimization toolbox for MATLAB*, 2004.
- ²²Lofberg, J., “YALMIP : A Toolbox for Modeling and Optimization in MATLAB,” *Proceedings of the CACSD Conference*, Taipei, Taiwan, 2004.
- ²³Balas, G., Packard, A., Seiler, P., and Topcu, U., “Robustness Analysis of Nonlinear Systems,” <http://aem.umn.edu/~AerospaceControl/>.
- ²⁴Dorobantu, A., Seiler, P., and Balas, G., “Time Delay Margin Analysis Applied to Model Reference Adaptive Control,” *AIAA Guidance, Navigation, and Control Conference*, No. AIAA-2011-6437, 2011.
- ²⁵Dorobantu, A., *Time Delay Margin Analysis for Adaptive Flight Control Laws*, Master’s thesis, University of Minnesota, 2010.
- ²⁶Nguyen, N. and Summers, E., “On Time Delay Margin Estimation for Adaptive Control and Robust Modification Adaptive Laws,” *AIAA Guidance, Navigation, and Control Conference*, No. AIAA 2011-6438, 2011.
- ²⁷Dydek, Z., Annaswamy, A., and Lavretsky, E., “Adaptive Control and the NASA X-15-3 Flight Revisited,” *IEEE Control Systems*, Vol. 30, 2010, pp. 32–48.
- ²⁸Annaswamy, A., Jang, J., and Lavretsky, E., “Stability margins for adaptive controllers in the presence of time delay,” *AIAA Guidance, Navigation, and Control Conference*, No. AIAA 2008-6659, 2008.
- ²⁹Skogestad, S. and Postlethwaite, I., *Multivariable Feedback Control*, John Wiley and Sons Ltd., 2007.
- ³⁰Powers, V. and Wörmann, T., “An Algorithm for Sums of Squares of Real Polynomials,” *Journal of Pure and Applied Algebra*, Vol. 127, 1998, pp. 99–104.
- ³¹Sturm, J., “SeDuMi version 1.05,” <http://fewcal.kub.nl/sturm/software/sedumi.html>, 2001.
- ³²Sturm, J., “Using SeDuMi 1.02, a MATLAB toolbox for optimization over symmetric cones,” *Optimization Methods and Software*, 1999, pp. 625–653.
- ³³Gatermann, K. and Parrilo, P., “Symmetry Groups, Semidefinite Programs, and Sums of Squares,” *Journal of Pure and Applied Algebra*, Vol. 192, 2004, pp. 95–128.
- ³⁴Ogata, K., *Modern Control Engineering*, Prentice Hall, 4th ed., 2002.
- ³⁵MATLAB, *version 7.8.0.347 (R2009a)*, The MathWorks Inc., Natick, MA, 2009.